

# Volcanic ash leaching as a means of tracing the environmental impact of the 2011 Grímsvötn eruption, Iceland

J. Cabré<sup>1,2</sup> · M. Aulinas<sup>2</sup> · M. Rejas<sup>1</sup> · J. L. Fernandez-Turiel<sup>1</sup>

Received: 13 October 2015 / Accepted: 24 March 2016 / Published online: 8 April 2016  
© Springer-Verlag Berlin Heidelberg 2016

**Abstract** The Grímsvötn volcanic eruption, from 21 to 28 May, 2011, was the largest eruption of the Grímsvötn Volcanic System since 1873, with a Volcanic Explosivity Index (VEI) of magnitude 4. The main geochemical features of the potential environmental impact of the volcanic ash-water interaction were determined using two different leaching methods as proxies (batch and vertical flow-through column experiments). Ash consists of glass with minor amounts of plagioclase, clinopyroxene, diopside, olivine and iron sulphide; this latter mineral phase is very rare in juvenile ash. Ash grain morphology and size reflect the intense interaction of magma and water during eruption. Batch and column leaching tests in deionised water indicate that Na, K, Ca, Mg, Si, Cl, S and F had the highest potential geochemical fluxes to the environment. Release of various elements from volcanic ash took place immediately through dissolution of soluble salts from the ash surface. Element solubilities of Grímsvötn ash regarding bulk ash composition were <1 %.

Combining the element solubilities and the total estimated mass of tephra ( $7.29 \times 10^{14}$  g), the total inputs of environmentally important elements were estimated to be  $8.91 \times 10^9$  g Ca,  $7.02 \times 10^9$  g S,  $1.10 \times 10^9$  g Cl,  $9.91 \times 10^8$  g Mg,  $9.91 \times 10^8$  g Fe and  $1.45 \times 10^8$  g P. The potential environmental problems were mainly associated with the release of F ( $5.19 \times 10^9$  g).

**Keywords** Volcanic ash · Water leaching · Geochemical flux · Grímsvötn

## Introduction

Explosive volcanic eruptions produce mixtures of particulate matter (tephra) and gases that are directly injected into the atmosphere. The interaction of tephra particles with the environment may induce a range of positive and negative physical, chemical and biological effects from local to global scales (Ayrís and Delmelle 2012). It is well known that eruptive columns reaching tropospheric and stratospheric heights can have detrimental consequences for the climate, including an increase in greenhouse gases, sulphur and halogen species, as well as aerosols, which could lead to the acidification of precipitation (Robock 2000; Fontijn et al. 2014; Long et al. 2014). On the other hand, volatiles released during an explosive volcanic eruption are usually adsorbed onto the surface of volcanic ash particles as water-soluble compounds (Rose 1977; Ayrís and Delmelle 2012). Scavenging of volatiles is variable, with the main elements being sulphur, chlorine and fluorine (Delmelle et al. 2007). After deposition, the adsorbed compounds can be released to the environment where they have the potential to damage water quality, vegetation, livestock and people, although, in some cases, these effects may be positive, e.g. fertilising lands and oceans (Weaire and Manly 1996; Duggen et al. 2010; Frogner et al. 2001;

Responsible editor: Philippe Garrigues

**Electronic supplementary material** The online version of this article (doi:10.1007/s11356-016-6559-7) contains supplementary material, which is available to authorized users.

✉ J. Cabré  
josep.cabre.brullas@gmail.com

J. L. Fernandez-Turiel  
jlfernandez@ictja.csic.es

<sup>1</sup> Institute of Earth Sciences Jaume Almera, ICTJA-CSIC, Lluís Solé i Sabarís s/n, 08028 Barcelona, Spain

<sup>2</sup> Departament de Geoquímica, Petrologia i Prospecció Geològica, Universitat de Barcelona, Martí i Franquès, s/n, 08028 Barcelona, Spain

Langmann et al. 2010; Witham et al. 2005). An important factor of such compounds is that they dissolve rapidly in contact with water (Olgun et al. 2011; Ayris and Delmelle 2012; Ruggieri et al. 2012a, b).

Other potential human impacts generated by the emission of tephra into the atmosphere include respiratory health hazards for the local population (Horwell and Baxter 2006; Horwell et al. 2013), as well as severe problems for aviation (Casadevall 1994; Guffanti et al. 2009). Recent examples of environmental and social impacts of volcanic particulate matter are found in the 2010 Eyjafjallajökull and 2011 Grímsvötn (Iceland) eruptions. Both generated a low impact globally, although they caused great disruption to air traffic across Europe, especially the 2010 Eyjafjallajökull eruption (Webster et al. 2012; Witham et al. 2012), and direct effects in Iceland as a result of the ash fall, such as physical damage to roads and bridges, impact on health and loss of crops (Horwell et al. 2013).

The aim of this work is to assess the main geochemical features of the environmental impact of volcanic ash-water interaction using the results of different leaching methods as proxies, through an analysis of the May 2011 Grímsvötn eruption. This work complements the findings of previous studies on this recent volcanic eruption (Oskarsson and Sverrisdóttir 2011; Horwell et al. 2013; Olsson et al. 2013; Sigmarsson et al. 2013), through the analysis of a distinct set of samples and the use of distinct leaching methodologies from previous works on the same eruption, allowing to determine more accurately the potential geochemical fluxes associated with the interaction of volcanic ash with water.

### Geological setting

The active Grímsvötn volcanic system (GVS) is aligned along a NE-SW fissure system in south-central Iceland which lies partly beneath the vast Vatnajökull icecap (Fig. 1). Grímsvötn central volcano is located above the Iceland mantle plume and thus has the highest rate of magma supply along the GVS. Laki fissure is located within the ice-free section of the GVS; in 1783–1784, it produced the largest historic lava flow on Earth, erupting about 14.7 km<sup>3</sup> of lava and ejecting 0.4 km<sup>3</sup> of dense-rock equivalent volume ( $V_{DRE}$ ) of tephra (Thordarson and Self 2003). The most recent events in the GVS are the 1996 Gjalp subglacial fissure eruption (Gudmundsson et al. 1997) and the smaller eruptions of 1998 (Sturkell et al. 2003) and 2004 (Jude-Eton et al. 2012). During an eruption, the extensive geothermal activity beneath the Vatnajökull icecap and the subglacial lake bound to the main caldera (Agustsdóttir and Brantley 1994; Alfaro et al. 2007) can enhance magma-water interactions (phreatomagmatic eruption) generating a tephra-laden plume that can rise rapidly to the upper troposphere.

The Grímsvötn eruption, which started approximately at 17:30 UTC on 21 May, 2011, was accompanied by an

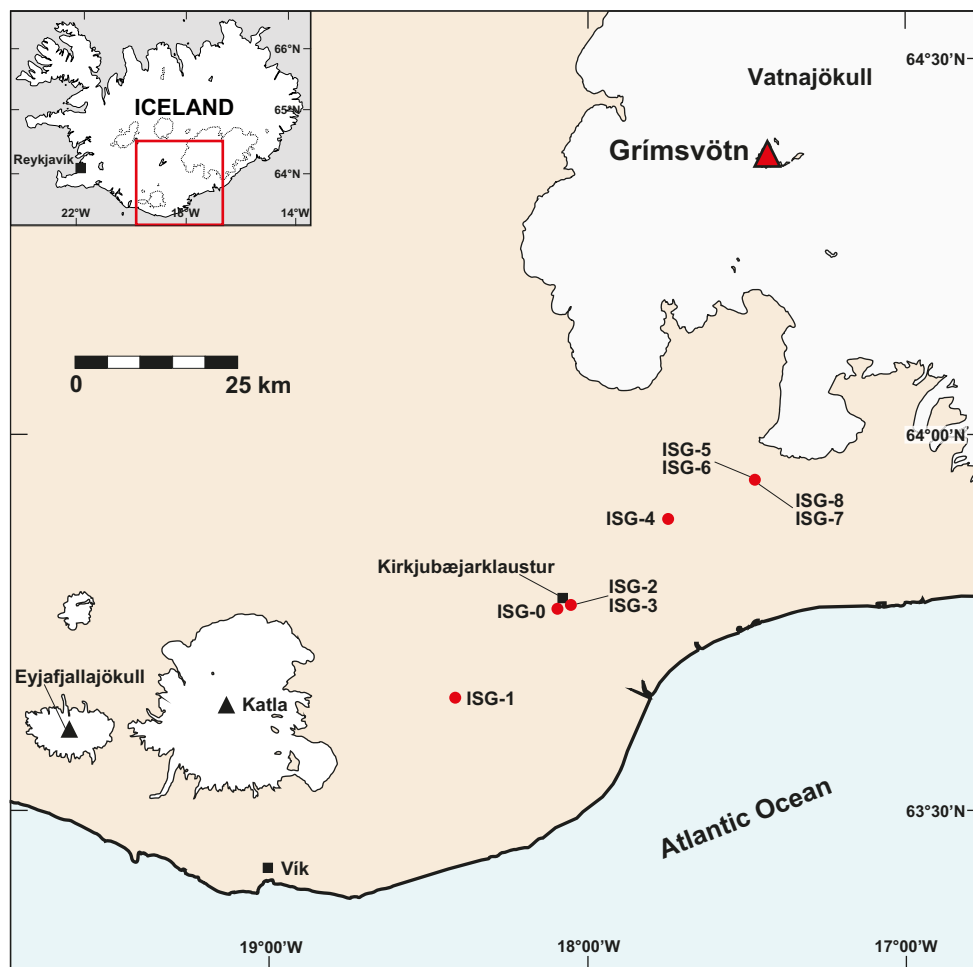
earthquake swarm. The highest eruptive intensity was recorded a few hours after the onset of the eruption when the plume reached a maximum altitude of 20–25 km (Petersen et al. 2012; Hreinsdóttir et al. 2014). After 24 h, the ash plume had reached about 100 km to the SW, affecting the villages of Kirkjubærklaustur and Vík (Fig. 1). Visibility in this area during the first few hours was extremely poor. In the following days, winds spread the ash plume over Iceland and distal fall-out was even observed in the British Isles, Scandinavia (Kerminen et al. 2011; Tesche et al. 2012) and Baltic countries (Kvietkus et al. 2013). After the first 24 h of the eruption, the volcanic plume decreased gradually, reaching heights closer to 10 km. On 23 May, the height of the plume decreased to 5 km, and on 28 May, the volcanic tremors rapidly decreased and finally disappeared at 07:00 UTC (Hreinsdóttir et al. 2014). The 21–28 May 2011 eruption was Grímsvötn's largest since 1873, with a Volcanic Explosivity Index (VEI) of magnitude 4 (Hreinsdóttir et al. 2014), thus representing a high potential risk through releasing various elements into water, specially fluorine, which can cause diseases in both animals and humans. Although this volcanic event caused some disruption to European airspace, it was minor compared to the 2010 Eyjafjallajökull eruption.

### Methods

Fieldwork was conducted across affected regions of southwestern Iceland on 22 and 25 May, 2011. Most of the ash was released from Grímsvötn before 23 May (Petersen et al. 2012; Olsson et al. 2013); thus, sample ISG-0 (Table 1), collected on 22 May at 14:02 UTC, might not contain volcanic ash from the paroxysmal phases of the eruption. The rest of the samples (eight) were collected on 25 May, from 14:32 to 18:27 UTC. It should be noted that, sometimes, it was slightly rainy during sampling on 25 May. Accordingly, the sampled ash from this day probably underwent some interaction with water, and therefore, we classify these samples as fresh rather than pristine. Sampling was carried out along a 100-km transect across the dispersal axis, following the main road through southern Iceland (Fig. 1). This work thus focuses on the effects of the eruption over the downwind region. The ash samples were collected at five sites located at different distances from the vent using a stainless steel shovel (Table 1 and Figs. 1 and 2). Once collected, they were placed in polyethylene bags and transported to the laboratory in which they were dried at 40 °C for 24 h in an oven and stored in polyethylene vessels until analysis.

Particle size distribution was obtained by laser diffractometry. Morphology and chemistry of ash particles were studied by scanning electron microscope (SEM). Mineralogy was determined by X-ray diffraction (XRD). Concentrations of major and trace elements in bulk ash samples and leachates were

**Fig. 1** Map showing the locations of volcanic ash samples, Grímsvötn volcano and other active volcanoes in southern Iceland, icecaps and urban areas



determined by high-resolution inductively coupled plasma-mass spectrometry (HR-ICP-MS). Additional information on analytical methods is provided in the ESM 1: supplementary material.

The volcanic ash leaching experiments were carried out using two independent methods, including a series of batch leaching tests and a flow-through column leaching test. In the batch experiments, 1 g of each ash sample was mixed with 10 ml of Milli-Q Plus ultrapure water type (18.2 M $\Omega$ /cm) in 14  $\times$  100-mm polypropylene test tubes (Ruggieri et al. 2012a, b). Deionised water was chosen as the leachant because it allows a rapid screening of the potentially hazardous species leached from the ash (Witham et al. 2005) and the results are more reliable simulating the leaching by rainwater and are independent of the local surface and groundwater chemistry. The water leachates were shaken at 20 rpm for 4 h and subsequently filtered through polyvinylidene difluoride (PVDF) syringe filters with tube tips (Whatman, 25-mm diameter and 0.45- $\mu$ m pore size). Finally, 1 % (v/v) HNO<sub>3</sub> was added to bring the volume up to 100 ml. The pH and the specific conductivity (SC) of batch leachates were monitored by means of specific electrodes (Crison Multimeter MM40) immediately

after mixing the ash and the deionised water (pH<sub>0</sub> and SC<sub>0</sub>), and after shaking (pH<sub>f</sub> and SC<sub>f</sub>), prior to filtering. The methods used to determine major and trace elements by HR-ICP-MS analysis were based on a previous study (Fernandez-Turiel et al. 2000). Sulphur concentrations are expressed as SO<sub>4</sub><sup>2-</sup> in the leachates. Fluoride concentrations were determined in the batch leachates prior to filtering using an ion-selective electrode (ISE) for fluoride (Orion, Thermo Scientific).

For the flow-through column leaching test, an 8-cm-long and 2.25-cm<sup>2</sup> cross-sectional-area vertical column (Teledyne ISCO Ref. 69-3873-140) was filled with 10 g of the representative ISG-3 ash, as in previous studies (Ruggieri et al. 2012a). Column loading was carried out gradually, allowing the water to percolate through the ash but avoiding the development of air bubbles. A silica filter with an average pore size diameter of 60 Å was attached at the column inlet and outlet. A peristaltic pump (Miniplus 3, Gilson) at the head of the column ensured a constant and stable deionised flow of water (Milli-Q Plus type, 18.2 M $\Omega$ /cm) from top to bottom at an average discharge of 0.12 ml/min with ash-water contact time of around 150 min. A fraction collector (FC 204, Gilson) at the

**Table 1** Main features of the studied ash from the 2011 Grimsvötn eruption

	ISG-0	ISG-1	ISG-2	ISG-3	ISG-4	ISG-5	ISG-6	ISG-7	ISG-8
Latitude	63° 47' 22" N	63° 40' 18" N	63° 47' 38" N	63° 47' 38" N	63° 54' 40" N	63° 57' 23" N	63° 57' 23" N	63° 57' 23" N	63° 57' 23" N
Longitude	18° 03' 02" W	18° 24' 13" W	18° 02' 17" W	18° 02' 17" W	17° 43' 14" W	17° 26' 58" W	17° 26' 58" W	17° 26' 58" W	17° 26' 58" W
Location	Kirkjubæjarklaustur	Laki lava	Skafthá river (Kirkjubæjarklaustur)	Skafthá river (Kirkjubæjarklaustur)	Brunná river	Skeiðarársandur	Skeiðarársandur	Skeiðarársandur	Skeiðarársandur
Distance from the vent (km)	75	95	75	75	57	49	49	49	49
Thickness (cm)	2	0–4	8	30	24	25	10.5	10	0.5
Collection date	22 May 2011	25 May 2011	25 May 2011	25 May 2011	25 May 2011	25 May 2011	25 May 2011	25 May 2011	25 May 2011
Preservation	Pristine	Fresh	Fresh	Fresh	Fresh	Fresh	Fresh	Fresh	Fresh
Glass	a	a	a	a	a	a	a	a	a
Augite	nd	nd	nd	nd	nd	b	nd	nd	b
Anorthite	nd	nd	nd	nd	nd	c	nd	nd	c
Pyrite	nd	nd	nd	nd	d	nd	nd	nd	nd
SiO <sub>2</sub>	56.14	52.49	52.23	50.94	54.49	52.07	51.40	55.80	55.25
Al <sub>2</sub> O <sub>3</sub>	12.26	12.78	12.64	13.53	12.73	12.99	14.01	11.88	12.94
Fe <sub>2</sub> O <sub>3</sub> total	12.70	13.45	13.50	13.62	13.28	12.60	13.21	12.44	12.19
MnO	0.22	0.23	0.24	0.23	0.24	0.23	0.23	0.22	0.22
MgO	4.99	5.04	5.17	5.22	4.94	5.73	4.99	4.63	5.92
CaO	8.94	9.25	9.29	9.54	9.18	10.13	9.64	8.67	10.53
Na <sub>2</sub> O	2.72	2.81	2.99	2.93	2.85	2.70	2.74	2.64	2.55
K <sub>2</sub> O	0.47	0.49	0.49	0.50	0.51	0.43	0.47	0.47	0.42
TiO <sub>2</sub>	2.61	2.76	2.78	2.82	2.81	2.49	2.64	2.60	2.38
P <sub>2</sub> O <sub>5</sub>	0.38	0.39	0.38	0.38	0.38	0.32	0.37	0.35	0.29
LOI	−0.87	−0.76	−0.35	−0.36	−0.82	−0.69	−0.94	−1.04	0.12
Total	100.56	98.94	99.35	99.34	100.59	99.01	98.76	98.66	102.82
Li	6.11	6.40	6.38	6.43	6.44	5.60	6.03	5.83	5.57
Be	0.98	0.99	0.97	1.06	1.01	0.85	0.93	0.97	0.78
Sc	36.8	37.8	38.5	39.4	38.1	42.1	39.8	36.2	42.5
V	205	282	206	256	339	213	194	207	330
Cr	37.7	33.6	43.4	28.9	37.3	78.4	52.4	41.9	78.0
Co	36.5	37.5	37.4	38.7	37.8	39.6	37.9	35.7	39.3
Ni	35.9	35.6	37.2	37.7	35.9	47.8	39.7	35.1	53.5
Cu	92.1	92.3	92.3	93.4	91.2	108	96.1	86.8	118
Zn	104	114	101	106	104	111	101	98.3	95.6
Ga	17.6	18.2	17.9	18.0	17.9	18.2	18.1	17.2	17.9
Ge	1.65	1.32	1.65	1.66	1.23	1.79	1.74	1.57	1.46
As	0.24	0.16	0.33	0.36	0.11	0.18	0.21	0.25	0.11
Rb	8.58	8.85	8.89	8.99	8.85	7.60	8.30	8.49	8.27
Sr	195	202	209	216	212	198	205	195	202
Y	37.4	39.6	40.6	41.1	40.8	35.7	38.4	38.0	34.4
Zr	205	212	216	221	219	179	206	210	172
Nb	19.9	20.6	20.0	20.0	20.5	17.1	19.1	18.4	15.5
Mo	0.65	0.60	0.61	0.63	0.63	0.52	0.58	0.61	0.49
Sn	1.14	1.16	1.20	1.20	1.17	1.07	1.10	1.18	1.09
Sb	0.04	0.05	0.04	0.04	0.04	0.04	0.04	0.05	0.04
Cs	0.08	0.09	0.09	0.09	0.09	0.08	0.08	0.09	0.07
Ba	91.3	95.0	97.6	96.2	96.1	82.5	90.1	90.8	83.4
La	14.5	14.7	15.2	15.2	15.4	13.0	14.5	13.8	12.4

Table 1 (continued)

	ISG-0	ISG-1	ISG-2	ISG-3	ISG-4	ISG-5	ISG-6	ISG-7	ISG-8
Ce	34.2	36.1	36.7	36.0	36.6	31.2	33.8	34.2	29.0
Pr	4.89	5.11	5.07	5.15	5.23	4.32	4.79	4.83	4.18
Nd	22.1	23.4	23.7	24.1	24.1	20.0	22.6	22.3	19.0
Sm	6.06	6.41	6.48	6.69	6.48	5.53	6.14	6.06	5.57
Eu	1.85	1.95	1.96	1.98	1.98	1.74	1.85	1.78	1.70
Gd	6.59	6.98	6.99	7.23	7.21	6.08	6.72	6.62	6.08
Tb	1.04	1.08	1.11	1.14	1.11	0.97	1.05	1.05	0.96
Dy	6.75	6.92	7.12	7.08	7.15	6.21	6.66	6.65	6.20
Ho	1.16	1.21	1.20	1.23	1.24	1.09	1.17	1.13	1.08
Er	3.40	3.60	3.67	3.68	3.72	3.26	3.42	3.40	3.19
Tm	0.57	0.60	0.61	0.62	0.62	0.55	0.58	0.58	0.54
Yb	3.42	3.57	3.68	3.69	3.69	3.21	3.47	3.44	3.18
Lu	0.53	0.55	0.57	0.57	0.56	0.48	0.52	0.52	0.49
Hf	4.08	4.17	4.11	4.12	4.29	3.52	3.99	3.94	3.45
Ta	1.01	1.03	1.00	1.04	1.07	0.85	0.93	0.95	0.82
W	0.22	0.22	0.22	0.22	0.22	0.19	0.21	0.49	0.19
Tl	0.02	0.02	0.02	0.02	0.02	0.02	0.02	0.02	0.02
Pb	1.28	1.25	1.32	1.24	1.21	1.21	1.40	1.14	1.18
Bi	0.01	0.01	0.02	0.01	0.01	0.01	0.01	0.01	0.01
Th	1.22	1.28	1.32	1.31	1.31	1.11	1.20	1.22	1.12
U	0.36	0.39	0.39	0.39	0.40	0.33	0.35	0.36	0.32

Major oxides and loss on ignition (LOI) expressed as %, m/m (mass/mass). Trace elements expressed as microgram per gram  
*nd* not detected

<sup>a</sup>Mineral compositions: prevalent

<sup>b</sup>Mineral compositions: common

<sup>c</sup>Mineral compositions: frequent

<sup>d</sup>Mineral compositions: scarce

column outlet directed samples from the leaching solution into 14 × 100-mm polypropylene test tubes. We employed the drop mode collection, counting 400 drops per tube of aqueous solution from the column outlet. One litre of percolated solution was collected in 6 days, resulting in a set of 100 tube samples. A subset of 37 samples was analysed for major and trace elements by HR-ICP-MS, based on a previous study (Fernandez-Turiel et al. 2000) using acidified (1 % HNO<sub>3</sub>) dilutions of 1:10 ml, v/v, with Milli-Q Plus-type deionised water. Another subset of 39 samples was analysed for pH and SC (Crison Multimeter MM40) immediately after tube filling. Samples were stored at 4 °C until analysis.

### Results and discussion

A total of nine samples were collected along the main plume dispersion axis. The ash fall deposited a practically continuous grey to dark grey blanket up to ~100 km to the SW of the Grímsvötn vent in Iceland. A maximum thickness of 30 cm was observed 75 km from the vent in the Skaftá riverbank near Kirkjubæjarklaustur (sampling site ISG-3, Fig. 2). The closest ash fall deposits to the eruptive focus showed two beds separated by a planar boundary. The lower bed had planar lamination (Fig. 2a). Sample ISG-7 was collected from the thicker ash layer (10 cm) in the lower section of the tephra deposit, whereas ISG-8 was collected from the thinner ash layer (0.5 cm) in the upper section (Fig. 2a). Samples ISG-5 (top) and ISG-6 (bottom) were collected a few meters from the previous outcrop where this two-layer structure was less clear. The rest of the samples were collected from deposits with no evidence of bedding or lamination (Fig. 2b–d).

The composition of the 2011 Grímsvötn ash ranged from basaltic to basaltic andesite, with silica content ranging from 50.94 to 56.14 %, m/m (Table 1). The samples are fairly homogeneous in terms of major oxide composition (Table 1), with a broader compositional range for the trace elements. The highest variation coefficients (20–50 %) were shown by V, Cr, As and W.

The particle size distribution of the volcanic ash deposits allows two main groups of samples to be distinguished (Fig. 3). The first group consists of unimodal and bimodal size distribution samples, although the dominant modes of the latter group are similar to those of the unimodal size distribution. The size distributions of ash with a maximum of between 72 and 125 µm show that the finer modes are in the more distal outcrops. The second group contains a bimodal distribution, with the dominant mode (753 µm) being coarser than that observed in the previous group (ISG-8) (Fig. 3b). The difference in particle size distribution might be related to variations in fragmentation associated with fluctuations in the volume of water interacting with magma; the ash is finer when the water content increases (Liu et al. 2015). Thus, water might have

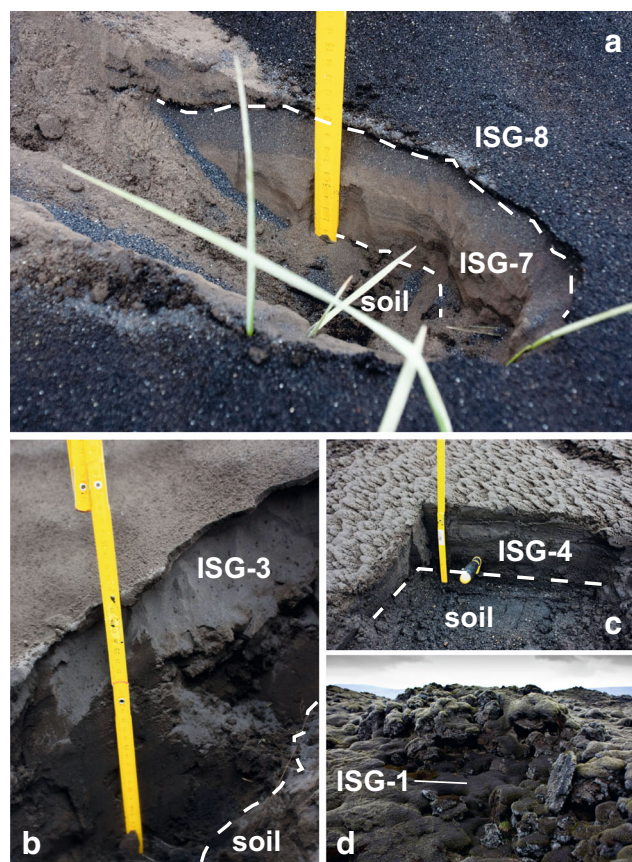


**Fig. 2** Photographs showing the ash sampling sites located at different distances from Grímsvötn volcano including **a** the most proximal to vent ash fall deposit sampled (49 km), with two beds; the *lower part* shows parallel lamination. **b** Massive deposit at site ISG-3, with the maximum thickness observed (30 cm), at 75 km from the vent in the Skaftá riverbank near Kirkjubæjarklaustur; the *upper part* was slightly hardened. **c** Massive deposit on the Brunná riverbank (57 km from the vent). **d** Laki lava lightly covered by ash (95 km from the vent)

played a lesser role during the last eruptive period, causing the magma to fragment into coarser ash (sample ISG-8). The origin of the polymodal distribution of ISG-5 is not clear but could be related to plume transport or wind reworking. Another application for particle size analysis of volcanic ash is the assessment of potential breathing hazards. ‘Thoracic’ or PM<sub>10</sub> (<10 µm) particles are likely to cause respiratory diseases, and ‘respirable’ or PM<sub>4</sub> (<4 µm) particles can have the greatest toxic potential (Horwell and Baxter 2006). The particle size analysis of the Grímsvötn ash showed ≤2.7 vol % for <4 µm and ≤6.0 vol % for 10 µm, which is consistent with the previous studies performed with different ash samples from the same eruption (<3.5 vol % <4 µm and <8.4 vol % <10 µm) (Horwell et al. 2013). In comparison, in the 2010 Eyjafjallajökull eruption, it has been found higher percentages of thoracic and respirable particles (2–13 vol % for <4 µm and 4–26 vol % for <10 µm), varying with the eruptive phase (Horwell et al. 2013). Taking into account the population density of southern Iceland (<3

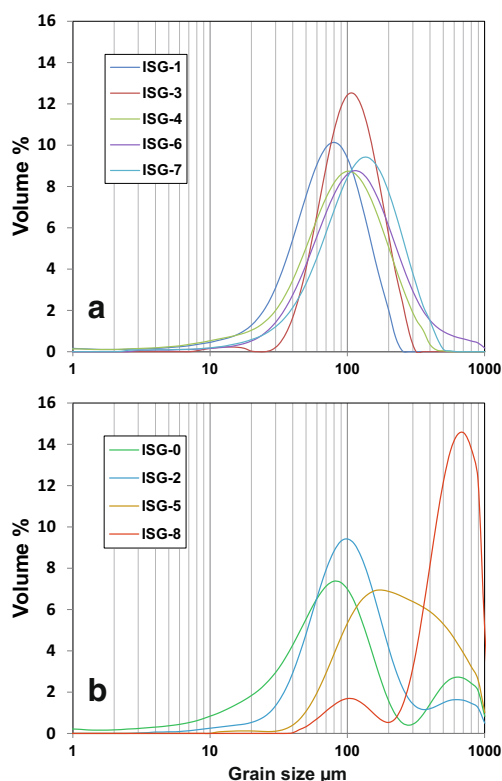


**Fig. 3** Particle size distribution of Grímsvötn 2011 ash of **a** samples with unimodal distribution and **b** samples with bimodal and polymodal distribution

inhabitants/km<sup>2</sup>) (EEA 2010) and the exposure time (8 days), the respiratory health risk of the Grímsvötn ash was low during the eruption and lower still than for the 2010 Eyjafjallajökull eruption.

Based on SEM and XRD analyses, the 2011 Grímsvötn ash has >90 % juvenile glass particles. The glass is associated with plagioclase, clinopyroxene, diopside and olivine phenocrysts. This mineralogical composition is coherent with data from previous studies on the erupted 2011 Grímsvötn ash (Olsson et al. 2013; Sigmarsson et al. 2013). An iron sulphide was also present as a minor phase (stoichiometric calculations were made assuming pyrite as the mineral phase observed), which was detected in the XRD measurements for the sample ISG-4. Although some rare occurrences of sulphide globules were indicated previously in Grímsvötn 2011 ash (Sigmarsson et al. 2013), the presence of iron sulphides, which are highly soluble in water, is presented for first time in this study.

General and detailed SEM images show that blocky shards are very angular and poorly to nonvesicular with curvilinear breakage surfaces (Fig. 4a, b). More rarely, fluidal particles with elongate vesicles (Fig. 4b) and spherical shapes (Fig. 4c) were found. Minor phases such as plagioclase, clinopyroxene, diopside and olivine are difficult to identify using the SEM because glass usually surrounds these crystals. Instead, iron sulphide formed subspherical aggregates of subhedral cubic crystals, partially covered by or free of glass (Fig. 4d). The

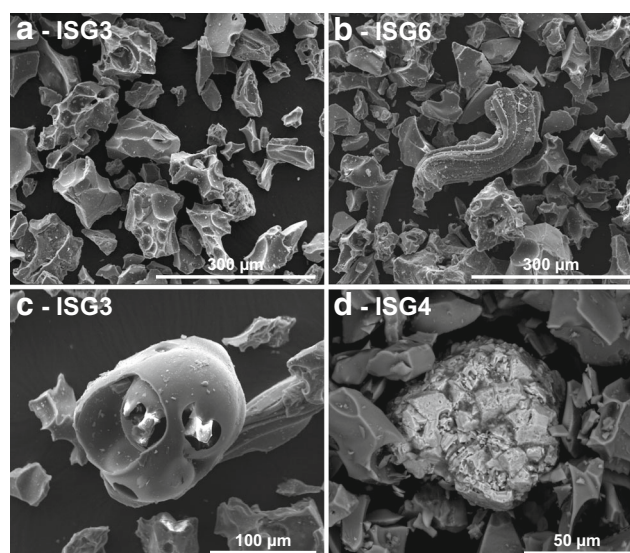


**Fig. 4** SEM images of the studied ash from the 2011 Grímsvötn eruption. Blocky shards are very angular and poorly to nonvesicular with curvilinear breakage surfaces (**a**, **b**). More scarcely, we found fluidal particles with elongate vesicles (**b**) and spherical shapes (**c**). **d** An iron sulphide. Images **a–c** were captured with an Everhart-Thomley detector (ETD), whereas **d** was taken with a back-scattered electron detector (BSED). **a**, **c** Sample ISG3. **b** Sample ISG6. **d** Sample ISG4

origin of this iron sulphide is probably the same as that proposed for the sulphide globules, i.e. generated by basalt-sulphide melt exsolution before degassing of the magma (Sigmarsson et al. 2013). The rim textures vary, probably related to differences in cooling rates.

The observed ensemble of shard morphologies is due to the explosive interaction of magma with water that favoured the particle fragmentation. Ash particle aggregates are scarce and could be associated with processes of early ash aggregation in the plume (Bonadonna et al. 2011; Taddeucci et al. 2011). This feature is expressed as bimodality in the particle size distribution of some samples (Fig. 3). However, due to the high water content and the height of the eruption column, more aggregates were expected to be found (Brown et al. 2012). This scarcity of aggregates could be related to the break-up of aggregate during ash fall, as in the 2010 Eyjafjallajökull eruption (Taddeucci et al. 2011).

We tried to obtain some proxies for the chemical processes occurring during the interaction of ash and water by means of the batch leaching experiments. This is a simple and fast way to establish the leaching rates of the elements during this interaction. A key question at this point is the ‘pristineness’ of the volcanic ash. Ash samples collected after or during rainfall are different to ash collected under dry conditions due to mobilisation of different salts from ash at different rates during the initial ash-water interaction (Taylor and Lichte 1980; Jones and Gislason 2008; Ruggieri et al. 2012a). Accordingly, leachate data might be compromised by rainfall in samples ISG-1 to ISG-8, leading to our classification of them as fresh rather than

pristine. In consequence, the results presented in this work must not be taken as ‘absolute’ fluxes of the eruption; however, they fingerprint the 2011 Grímsvötn eruption and indicate the order of magnitude of the fluxes involved.

Results of the single batch leaching tests showed a water-leach solution which was slightly acidic immediately after the ash-water interaction, with the exception of three samples which were weakly alkaline, ranging from pH 5.80 to 7.62 (Table 2). After shaking for 4 h, the average pH of leachates increased by around 1.90 pH units, resulting in solutions whose pH ranged between 7.33 and 9.26. This increase can be explained by ionic exchange, i.e. dissolution of surface cations and protons of glass and minerals (Gislason and Oelkers 2003; Ruggieri et al. 2010). The behaviour of the explosive ash from Eyjafjallajökull in 2010 was similar, with a slightly more basic pH (pH~8) which rose after the ash-water mixing (Gislason et al. 2011). The initial values of specific conductivity (SC) ranged from 7 to 356  $\mu\text{S}/\text{cm}$  (Gislason et al. 2011), increasing in all samples in the final solutions to a range of 14–404  $\mu\text{S}/\text{cm}$  (Table 2). The samples with lower values of pH and SC were ISG-5 and ISG-8, the coarser samples and probably more affected by rain (Table 2 and Fig. 3).

When the batch results of this work are compared with data from other tephra-leachate studies (Ayrís and Delmelle 2012), the Grímsvötn leaching results are at the lower end of the ranges, with clearly lower means and medians, even taking into account the rain effect and the differences in leaching methodologies. The Grímsvötn leaching results are in agreement with the observations in previous works (Ruggieri et al. 2012b; Witham et al. 2012; Olsson et al. 2013).

Table 3 compares the batch leached fraction of a Grímsvötn ash (sample ISG-3) with Chaitén 2008 eruption (Chile) and Eyjafjallajökull 2010 eruption (Iceland). The 2008 Chaitén eruption (Ruggieri et al. 2012a) was rhyolitic in composition and is located in a different geological setting, but the batch test was carried out following the same methodology as the one used for the 2011 Grímsvötn ash. In contrast, the 2010 Eyjafjallajökull eruption was compositionally closer to Grímsvötn, and both were located in the same geotectonic setting. However, these samples of the phase I eruption were not pristine, and the solute/ash ratio (1:25), agitation type and time (2 h) used in the batch test were different (Bagnato et al. 2013).

Despite the differences, their leached fractions produce similar results in terms of order of magnitude for major elements. The exceptions are Cl and K, which are exceptionally low in the Grímsvötn ash. The remarkably low release of Cl was also found in column leachates (Olsson et al. 2013). Overall, minor and trace elements are leached at lower rates in the Grímsvötn than in the Chaitén and Eyjafjallajökull ashes.

A proxy for the mobility of elements during the ash-water interaction is the relative mass leached (RML) which is defined as the percentage of the element that can be mobilised through

ash-water interaction, and it is expressed as the fraction of the leached element obtained from the batch experiment ( $\text{Conc}_{\text{batch}}$ ) over the element’s bulk concentration ( $\text{Conc}_{\text{bulk}}$ ). Therefore, RML is expressed as  $\text{RML \%} = \text{Conc}_{\text{batch}} / \text{Conc}_{\text{bulk}} * 100$  (Table 3).

To determine the leached mass for each element, we need to know the total mass of tephra erupted in 2011 by Grímsvötn volcano, which can be estimated using the dense-rock equivalent volume ( $V_{\text{DRE}}$ ) and the density ( $\rho_{\text{DRE}}$ ). The  $V_{\text{DRE}}$  expresses the volume without the void spaces in the ash particles (vesicles) and the interparticle space. The  $V_{\text{DRE}}$  was estimated as being  $0.27 \pm 0.07 \text{ km}^3$  for this eruption (Hreinsdóttir et al. 2014). Assuming a  $\rho_{\text{DRE}}$  of  $2700 \text{ kg}/\text{m}^3$ , the resulting mass is  $7.29 \times 10^{14} \text{ g}$ . The results obtained for the studied elements are in Table 3.

Each element was classified arbitrarily according to their RML mobility proxy, differentiating between elements with moderate (RML 0.5 to 1.00 %; Sn), low (0.01 to 0.5 %; As, Bi, W, Pb, Sb, Tl, Li, Mo, Zn, Na, Cu, K, Cs, Ca, Sr, Ni, P, Be, Rb, Tb and Ta) and very low mobility (RML < 0.01 %; Ge, rare earth elements or REE, Th, Y, Ba, Mg, Mn, Ga, Al, Hf, V, Cr, Co, Fe, Nb, Sc, U, Zr, Ti, Si and Ag). The results show a small degree of mobility for all elements and remarkably low for major elements. Although the concentrations of Cl, S, B, F, Se, Br, Cd, I and Hg were analysed in the batch experiments, their RML could not be estimated since their bulk compositions were not determined. Despite the low mobility of elements, the overall quantity released into water may be sizeable (Table 3) by combining the element solubilities and the total estimated mass of tephra. Grímsvötn ash contains notable contents of potential macronutrients ( $8.91 \times 10^9 \text{ g Ca}$ ,  $7.02 \times 10^9 \text{ g S}$ ,  $9.91 \times 10^8 \text{ g Mg}$  and  $1.45 \times 10^8 \text{ g P}$ ) and micronutrients ( $1.10 \times 10^9 \text{ g Cl}$  and  $9.91 \times 10^8 \text{ g Fe}$ ) for biological processes, which show the fertilising potential of the ash both in terrestrial ecosystems (Weaire and Manly 1996) and in the surface water of oceans (Duggen et al. 2010; Olgun et al. 2013). Although these values give an estimation of the impacts on marine environment, a leachate study using natural seawater would determine more precisely the impact of the Grímsvötn ash in oceanic waters. Potential environmental problems arising from ash fallout on land or into fresh water systems, on the other hand, are mainly associated with the release of fluoride ( $5.19 \times 10^9 \text{ g F}$ ), with the hazard of other potentially toxic elements or compounds being extremely low in comparison. It can be observed when contrasting the potential leachable mass of the 2010 Eyjafjallajökull (Bagnato et al. 2013; Gudmundsson et al. 2012) with the 2011 Grímsvötn eruption that the potential release of macronutrients ( $4.79 \times 10^{10} \text{ g Ca}$ ,  $1.48 \times 10^{10} \text{ g S}$ ,  $2.63 \times 10^9 \text{ g Mg}$ ) and Cl ( $5.57 \times 10^{10} \text{ g}$ ) to the environment for the former ash was higher, except for Fe ( $3.65 \times 10^8$ ). The potential leachable mass of fluoride in the 2010 eruption was also higher ( $1.53 \times 10^{10} \text{ g}$ ) in the Eyjafjallajökull ash. The sulphur fluxes of the 2011 Grímsvötn eruption have been studied previously



**Table 2** pH and specific conductivity (SC) of the batch leaching tests of Grímsvötn samples which were monitored immediately after mixing the ash and the deionised water (pH<sub>0</sub> and SC<sub>0</sub>) and after 4-h shaking (pH<sub>f</sub> and SC<sub>f</sub>) without filtering

Parameter	Unit	ISG-0	ISG-1	ISG-2	ISG-3	ISG-4	ISG-5	ISG-6	ISG-7	ISG-8
pH <sub>0</sub>	pH unit	7.62	7.20	6.65	6.80	7.20	6.12	6.00	6.10	5.80
pH <sub>f</sub>	pH unit	8.93	8.84	7.75	8.22	9.26	7.68	8.17	8.84	7.33
SC <sub>0</sub>	μS/cm	90	117	356	101	43	18	86	96	7
SC <sub>f</sub>	μS/cm	244	148	404	122	100	28	110	130	15
Ca	mg/l	2.04	1.77	3.62	1.22	1.03	0.64	0.89	1.26	0.42
Mg	mg/l	0.23	0.16	0.54	0.14	0.11	0.10	0.13	0.13	0.06
Na	mg/l	1.39	0.80	2.41	0.71	0.58	0.25	0.70	0.72	0.24
K	mg/l	0.11	0.11	0.13	0.10	0.08	0.11	0.10	0.07	0.11
Si	mg/l	0.18	0.21	0.15	0.12	0.11	0.17	0.11	0.13	0.15
Cl	mg/l	0.29	0.15	0.54	0.15	0.11	0.10	0.13	0.15	0.10
SO <sub>4</sub>	mg/l	6.02	3.47	12.80	2.89	2.42	0.63	2.80	3.15	0.34
F	mg/l	1.73	0.90	1.37	0.71	0.81	0.08	0.58	0.88	0.02
Li	μg/l	0.61	0.39	0.81	0.30	0.27	0.11	0.34	0.33	0.11
Be	μg/l	0.01	0.02	0.01	0.01	0.01	0.01	0.01	0.01	0.02
B	μg/l	27.6	26.0	17.2	17.9	19.3	24.3	29.2	17.8	27.2
Al	μg/l	180.7	372.5	188.4	168.1	201.7	264.3	223.6	183.4	272.7
P	μg/l	23.4	35.0	21.1	19.8	18.1	19.2	13.8	19.3	17.6
Sc	μg/l	0.07	0.11	0.06	0.06	0.06	0.08	0.05	0.06	0.06
Ti	μg/l	6.54	19.00	7.52	6.06	8.76	11.93	8.11	8.47	8.49
V	μg/l	0.91	1.50	0.72	0.63	0.71	0.65	0.57	0.80	0.62
Cr	μg/l	0.08	0.12	0.09	0.13	0.10	0.23	0.11	0.07	0.17
Fe	μg/l	173.9	382.9	187.8	135.9	173.6	195.1	138.8	184.6	130.7
Mn	μg/l	11.40	14.69	12.54	10.71	8.43	5.08	6.53	8.65	2.93
Co	μg/l	0.11	0.17	0.07	0.08	0.09	0.07	0.08	0.09	0.05
Ni	μg/l	0.66	0.79	0.52	0.80	0.57	0.39	0.56	0.48	0.72
Cu	μg/l	2.45	6.87	3.64	2.69	3.12	1.95	2.27	3.09	1.61
Zn	μg/l	4.29	5.11	4.94	5.21	3.70	4.00	3.70	3.12	7.07
Ga	μg/l	0.08	0.12	0.06	0.05	0.06	0.05	0.06	0.07	0.04
Ge	μg/l	0.02	0.02	0.02	0.01	0.01	0.02	0.02	0.01	0.01
As	μg/l	0.03	0.10	0.03	0.03	0.07	0.03	0.13	0.04	0.10
Se	μg/l	1.92	2.08	1.10	1.00	0.76	1.31	-0.21	1.33	1.46
Rb	μg/l	0.10	0.12	0.13	0.09	0.08	0.09	0.08	0.08	0.07
Sr	μg/l	4.89	3.85	8.00	2.92	2.33	2.05	2.06	2.90	1.22
Y	μg/l	0.36	0.51	0.33	0.27	0.25	0.35	0.17	0.29	0.23
Zr	μg/l	0.13	0.18	0.13	0.12	0.14	0.13	0.24	0.10	0.20
Nb	μg/l	0.04	0.04	0.04	0.04	0.03	0.04	0.04	0.03	0.04
Mo	μg/l	0.05	0.04	0.06	0.03	0.02	0.02	0.02	0.03	0.02
Ag	μg/l	0.02	0.02	0.02	0.03	0.02	0.02	0.02	0.01	0.02
Cd	μg/l	0.02	0.02	0.02	0.02	0.01	0.01	0.01	0.01	0.01
Sn	μg/l	0.95	0.86	1.05	1.31	0.80	1.10	0.87	0.60	0.96
Sb	μg/l	0.014	0.005	0.007	0.007	0.004	0.005	0.003	0.006	0.009
I	μg/l	0.27	0.29	0.24	0.22	0.19	0.22	0.20	0.18	0.19
Cs	μg/l	0.003	0.002	0.002	0.002	0.002	0.002	0.002	0.002	0.002
Ba	μg/l	0.67	0.67	0.68	0.57	0.45	0.60	0.47	0.44	0.52
La	μg/l	0.160	0.224	0.145	0.117	0.111	0.165	0.081	0.127	0.111
Ce	μg/l	0.387	0.526	0.313	0.274	0.260	0.356	0.185	0.303	0.240
Pr	μg/l	0.054	0.074	0.045	0.039	0.036	0.051	0.025	0.042	0.034
Nd	μg/l	0.253	0.359	0.211	0.174	0.173	0.249	0.122	0.203	0.164

**Table 2** (continued)

Parameter	Unit	ISG-0	ISG-1	ISG-2	ISG-3	ISG-4	ISG-5	ISG-6	ISG-7	ISG-8
Sm	µg/l	0.062	0.097	0.056	0.049	0.046	0.057	0.030	0.053	0.041
Eu	µg/l	0.022	0.029	0.019	0.014	0.014	0.018	0.010	0.017	0.012
Gd	µg/l	0.076	0.105	0.065	0.050	0.049	0.065	0.032	0.060	0.045
Tb	µg/l	0.014	0.018	0.012	0.010	0.009	0.013	0.007	0.011	0.008
Dy	µg/l	0.078	0.111	0.059	0.053	0.052	0.069	0.032	0.063	0.047
Ho	µg/l	0.014	0.019	0.012	0.010	0.009	0.012	0.006	0.011	0.009
Er	µg/l	0.038	0.055	0.034	0.026	0.026	0.036	0.017	0.031	0.025
Tm	µg/l	0.005	0.007	0.004	0.003	0.003	0.005	0.002	0.004	0.003
Yb	µg/l	0.031	0.041	0.024	0.021	0.020	0.028	0.014	0.024	0.020
Lu	µg/l	0.004	0.006	0.004	0.003	0.003	0.005	0.002	0.003	0.003
Hf	µg/l	0.017	0.017	0.012	0.011	0.011	0.011	0.015	0.011	0.013
Ta	µg/l	0.010	0.012	0.010	0.010	0.009	0.011	0.011	0.007	0.010
W	µg/l	0.06	0.06	0.06	0.12	0.06	0.07	0.06	0.04	0.06
Hg	µg/l	0.022	0.009	0.007	0.008	0.006	0.001	0.006	0.010	0.001
Tl	µg/l	0.003	0.004	0.003	0.003	0.003	0.003	0.003	0.002	0.003
Pb	µg/l	0.22	0.30	0.42	0.35	0.25	0.25	0.29	0.17	0.28
Bi	µg/l	0.004	0.004	0.003	0.003	0.003	0.003	0.003	0.003	0.003
Th	µg/l	0.013	0.013	0.013	0.008	0.008	0.008	0.010	0.009	0.008
U	µg/l	0.003	0.010	0.003	0.004	0.007	0.005	0.011	0.004	0.010

SC is expressed as microsiemens per centimetre

(Sigmarsson et al. 2013). These authors estimate that  $7.3 \times 10^{11}$  g of S was emitted during this eruption, which can be broken down to  $7.2 \times 10^{11}$  g of S as SO<sub>2</sub> gas detected by satellite (26 %),  $1.2 \times 10^{11}$  g of leachable S (16 %),  $3.7 \times 10^{10}$  g of S released in the Jöhulhlaups (5 %) and  $3.8 \times 10^{11}$  g of S in sulphide globules (53 %). The value obtained for the leachable S content was taken from previous estimations (Olsson et al. 2013). The leachable S value is notably lower in the present work, independent of the leaching method, probably due to prior leaching during rainfall. The results from both previous work and this study on sulphide estimates are equivalent to ~0.3 % of pyrite, which is coherent with our observations by XRD and SEM.

The flow-through column leaching test allows the evolution of the leached composition over time to be modelled. The test was carried out with sample ISG-3 due to its representativeness within the 2011 Grímsvötn eruption ash collection. Its selection was done following field and laboratory criteria. Firstly, it was one of the samples not visually affected by rain during sampling, and secondly, it is the sample with the most representative particle size distribution. The results are given in ESM 2: Table S1 (supplementary material) and Fig. 5, where they are plotted as progression curves of pH, major and trace elements versus accumulated volume of the percolated solution (Fig. 5).

The pH ranges from 6.55 to 7.10, increasing rapidly at the very beginning of the experiment. This trend has been

commonly reported in other volcanic ash column leaching tests (Rango et al. 2010; Ruggieri et al. 2010). Once pH has reached its maximum (7.10), the general trend is towards a progressive decrease for about 0.3 units from the beginning to the end, following a saw-tooth pattern. The initial rise in pH was also recognised in the batch experiment, and it is likely due to the virtually instantaneous exchange of the alkaline ion by H<sup>+</sup> (or as (H<sub>3</sub>O)<sup>+</sup>), i.e. increase in pH (Ruggieri et al. 2010). The concentrations of the elements in the percolated solution tend to decrease gradually through time. The high incipient concentrations of SO<sub>4</sub><sup>2-</sup>, Na, Ca, Mg, K and Sr (Fig. 5) confirm the presence of soluble compounds on ash particle surfaces, originating from interaction between tephra and volcanic gases within the eruption column (Rose 1977; Delmelle et al. 2007). A considerable number of elements show a major peak in concentration between 50 and 60 ml of percolated solution, which sometimes exceeds the initial concentrations (Si, Al, P, Ti, V, Fe, Ni, Cu, Zn, Zr and Ba). This anomaly in the decreasing trend may be due to the incongruent dissolution of volcanic glass by cation exchange processes (Rango et al. 2010; Ruggieri et al. 2010). Towards the end, the element concentrations become stable, suggesting that the most leachable fraction is exhausted. This situation is reached at relatively small percolated volumes for Na, Si and Cl (~150 ml), indicating a very fast release of these elements, while the stabilisation of element concentration for Ti, Mn and Zn is notably higher, by up to four times (~600 ml), indicating a more prolonged release over time.

**Table 3** Potential geochemical fluxes associated with the 2011 Grímsvötn eruption

Element	Batch leached fraction average					Batch leached fraction			Grímsvötn (2011)				
	Ayrís and Delmelle (2012)					Chaitén (2008)	Eyjafjallajökull (2010)	Grímsvötn (2011)	This work				
	mg/kg				Count	Ruggieri et al. (2012a, b)	Bagnato et al. (2013)	This work	Bulk mass	Leachable mass (batch)		Leachable mass (column)	
	Max	Min	Mean	Median		mg/kg	mg/kg	mg/kg	mt	mt	% of bulk (RML)	mt	% of batch
Ca	23,590	<1	2172	2140	27	80.0	99.8	12.22	49,299,716	8908	0.0181	2034	22.8
S	17,770	<1	1711	1662	30	51.1	30.9	9.63	nd	7021		973	13.9
Na	2560	<1	407	378	28	64.2	151	7.13	14,977,060	5198	0.0347	914	17.6
F	3140	<1	135	129	29	6.80	31.9	7.13	nd	5194		nd	
Al	1164	<1	63	58	24	4.95	1.79	1.68	49,623,245	1225	0.0025	446	36.4
Cl	11,160	5	1189	1162	30	148	116	1.50	nd	1094		140	12.8
Mg	4240	<1	349	335	27	6.57	5.47	1.36	22,780,688	991	0.0044	257	25.9
Fe	606	<1	24	21	24	<LoD	0.76	1.36	66,279,957	991	0.0015	374	37.8
Si	390	<1	27	25	24	18.4	nd	1.18	182,045,381	860	0.0005	817	95.0
K	788	<1	76	71	26	14.2	17.7	1.02	2,863,742	744	0.0260	82.2	11.1
P	724	<1	74	74	12	0.37	nd	0.20	1,145,187	145	0.0126	19.5	13.5
B	7.72	0.00	2.69	2.61	9	<LoD	0.05	0.18	nd	130		nd	
Mn	144	<1	22	20	22	0.47	0.46	0.107	1,291,854	78.1	0.0060	7.72	9.9
Ti	18.67	<0.001	2.32	2.32	12	0.09	0.05	0.061	11,601,750	44.1	0.0004	38.5	87.2
Zn	53.02	<0.10	4.01	3.58	21	0.17	0.42	0.052	75,643	38.0	0.0502	3.01	7.9
Sr	35.05	0.38	4.63	4.30	14	0.15	0.16	0.029	148,482	21.3	0.0143	4.16	19.6
Cu	95	<1	6	5	22	0.04	0.07	0.027	70,503	19.6	0.0278	1.05	5.3
Sn	0.119	0.008	0.079	0.079	11	nd	nd	0.013	835	9.51	1.1396	0.180	1.9
Se	0.550	<0.025	0.059	0.055	14	nd	0.01	0.010	nd	7.25		1.61	22.1
Ni	3.90	<0.10	0.52	0.50	14	0.05	0.03	0.008	29,038	5.85	0.0202	0.642	11.0
V	0.300	<0.10	0.091	0.089	14	0.01	0.05	0.006	180,735	4.57	0.0025	3.16	69.2
Ba	6.70	<0.10	0.94	0.94	14	0.09	0.05	0.006	66,662	4.16	0.0062	0.600	14.4
Pb	2.07	<0.050	0.14	0.11	16	0.35	0.008	0.003	908	2.53	0.2786	0.110	4.4
Li	1.88	<0.001	0.27	0.22	14	0.10	0.06	0.003	4438	2.18	0.0491	0.376	17.2
Ce	0.110	<0.010	0.063	0.063	5	0.00	nd	0.003	24,936	2.00	0.0080	0.119	6.0
Y	1.000	0.001	0.035	0.029	6	<LoD	nd	0.003	28,031	1.94	0.0069	0.111	5.7
I						nd	nd	0.002	nd	1.63		0.041	2.5
Nd	0.042	0.008	0.022	0.022	5	nd	nd	0.002	16,309	1.27	0.0078	0.076	6.0
Cr	0.52	<0.050	0.10	0.10	13	0.01	0.02	0.001	34,957	0.94	0.0027	0.289	30.8
Zr	<0.001	<0.001	0.0020	0.0020	6	0.01	nd	0.001	149,009	0.87	0.0006	0.281	32.4
La	0.200	<0.10	0.042	0.041	6	nd	nd	0.001	10,428	0.85	0.0082	0.050	5.9
W	0.0110	0.002	0.0060	0.0060	5	nd	nd	0.0012	178	0.85	0.4785	0.024	2.8
Rb	0.240	<0.015	0.083	0.083	6	0.03	nd	0.0009	6222	0.67	0.0108	0.076	11.4
Co	1.30	<0.010	0.20	0.19	16	<LoD	0.001	0.0008	27,578	0.60	0.0022	0.146	24.4
Sc						0.02	nd	0.0006	28,441	0.40	0.0014	0.092	22.9
Dy	0.0050	<0.001	0.0020	0.0020	5	nd	nd	0.0005	4919	0.39	0.0079	0.024	6.2
Gd	0.0070	<0.001	0.0040	0.0040	5	nd	nd	0.0005	4900	0.36	0.0074	0.021	5.7
Ga	0.033	0.006	0.013	0.013	5	nd	nd	0.0005	13,050	0.36	0.0027	0.197	55.3
Sm	0.0060	<0.001	0.0030	0.0030	5	nd	nd	0.0005	4489	0.36	0.0080	0.020	5.6
Pr	0.0100	<0.001	0.0050	0.0050	5	nd	nd	0.0004	3529	0.28	0.0081	0.016	5.7
Nb	<0.001	<0.001	<0.001	<0.001	5	0.05	nd	0.0004	13,864	0.26	0.0019	0.025	9.4
Mo	0.620	<0.040	0.069	0.063	12	0.02	0.02	0.0003	430	0.23	0.0543	0.036	15.5

**Table 3** (continued)

Element	Batch leached fraction average					Batch leached fraction			Grímsvötn (2011)				
	Ayrís and Delmelle (2012)					Chaitén (2008)	Eyjafjallajökull (2010)	Grímsvötn (2011)	This work				
	mg/kg				Count	Ruggieri et al. (2012a, b)	Bagnato et al. (2013)	This work	Bulk mass	Leachable mass (batch)		Leachable mass (column)	
	Max	Min	Mean	Median		mg/kg	mg/kg	mg/kg	mt	mt	% of bulk (RML)	mt	% of batch
Ag	1.0790	<0.001	0.0070	0.0010	5	nd	nd	0.0003	nd	0.23		0.012	5.5
Er	0.0020	<0.001	0.0010	0.0010	5	nd	nd	0.0003	2539	0.19	0.0075	0.013	6.8
As	9.33	<0.10	0.16	0.13	13	0.35	0.01	0.0003	158	0.18	0.1153	0.033	17.9
Yb	<0.001	<0.001	<0.001	<0.001	5	nd	nd	0.0002	2539	0.15	0.0060	0.010	6.8
Cd	0.337	<0.004	0.057	0.053	15	nd	0.002	0.00018	nd	0.13		0.007	5.1
Eu	<0.001	<0.001	0.0000	0.0000	5	nd	nd	0.0001	1361	0.10	0.0075	0.007	6.5
Ge	0.0080	<0.001	0.0030	0.0030	5	nd	nd	0.0001	1140	0.10	0.0090	0.034	32.9
Be	0.0160	<0.001	0.0050	0.0050	6	nd	nd	0.00011	692	0.080	0.0116	0.009	10.6
Hf	0.189	<0.001	0.079	0.079	5	nd	nd	0.00011	2890	0.08	0.0028	0.009	10.7
Ho	<0.001	<0.001	0.0010	0.0010	5	nd	nd	0.00010	851	0.073	0.0086	0.005	6.2
Ta	0.025	<0.001	0.010	0.010	5	nd	nd	0.00010	704	0.073	0.0104	0.004	5.9
Tb	<0.001	<0.001	0.0010	0.0010	5	nd	nd	0.00010	771	0.073	0.0095	0.004	5.7
Hg	0.0090	<0.001	0.0000	0.0000	11	nd	nd	0.00008	nd	0.058		0.003	5.7
Th	<0.001	<0.001	0.0010	0.0010	5	nd	0.0003	0.00008	898	0.058	0.0065	0.004	6.7
Sb	0.070	<0.010	0.024	0.024	7	0.00	0.001	0.00007	31	0.051	0.1662	0.005	9.8
U	0.0120	<0.001	0.0020	0.0020	9	nd	0.0004	0.00004	5739	0.029	0.0005	0.002	7.7
Bi	0.150	<0.005	0.014	0.015	11	nd	nd	0.00003	9	0.022	0.2523	0.002	7.3
Lu	<0.001	<0.001	<0.001	<0.001	5	nd	nd	0.00003	387	0.022	0.0057	0.002	7.6
Tl	0.1200	<0.001	0.0060	0.0040	7	nd	nd	0.00003	15	0.022	0.1467	0.002	7.8
Tm	<0.001	<0.001	0.0010	0.0010	5	nd	nd	0.00003	426	0.022	0.0051	0.002	8.1
Cs	0.033	0.001	0.008	0.008	5	0.00	0.0004	0.00002	62	0.015	0.0236	0.002	13.0

Data for batch (1 g volcanic ash was shaken with 10 ml of deionised water for 4 h) and column leaching (10-g ash was leached in a flow-through column with 1000 ml of deionised water pumped at 0.12 ml/min) experiments are shown for the same sample (ISG-3), chosen for its preservation and particle size distribution. Batch results are compared with an average of ash batch tests (Ayrís and Delmelle 2012), sample CH-1F of 2008 Chaitén eruption (Ruggieri et al. 2012a) and mean values of samples from the first eruptive phase of the 2010 Eyjafjallajökull eruption (Bagnato et al. 2013)

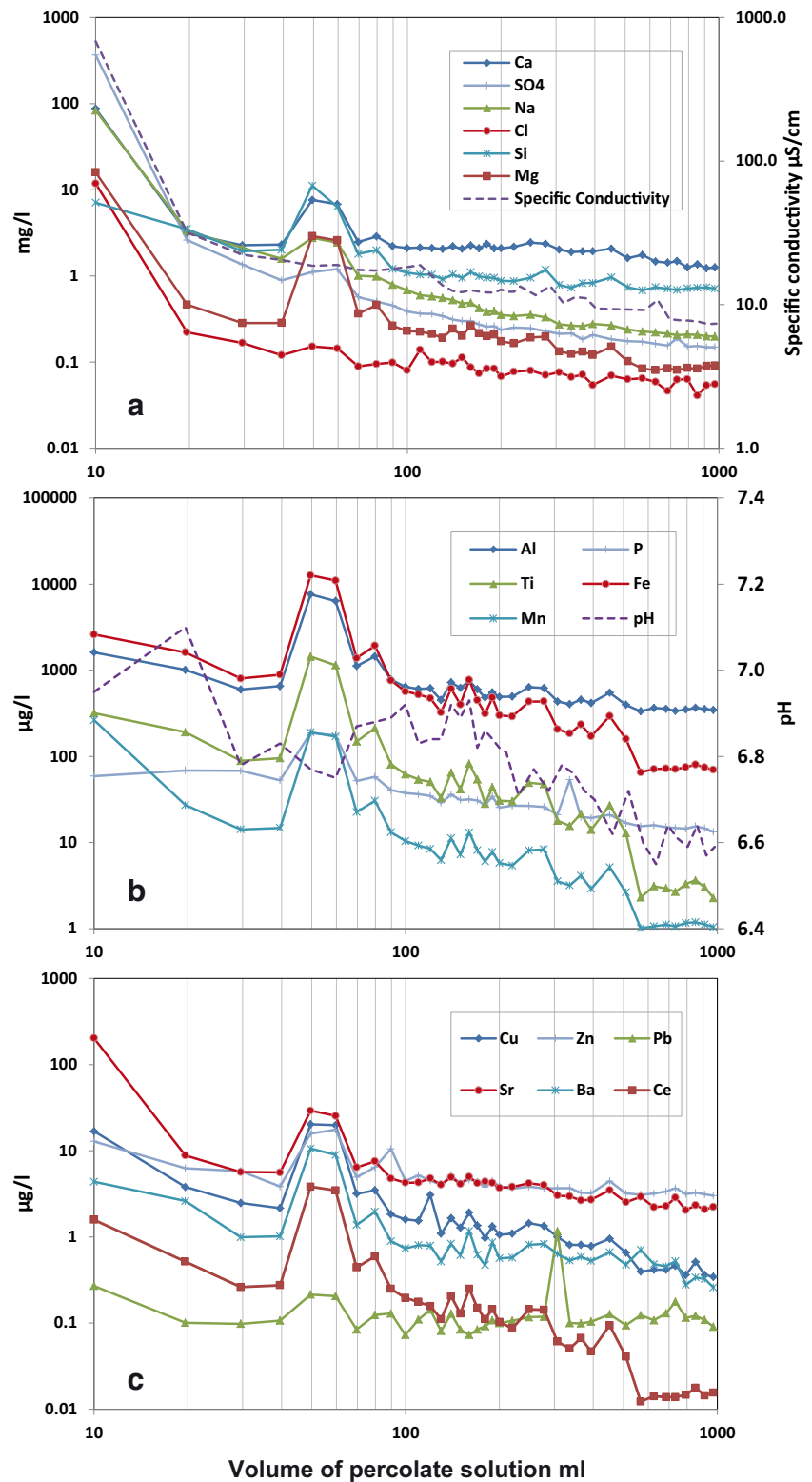
nd not determined, <LoD lower than limit of detection

When the discrete column leaching results are plotted on the Chadha diagram (Chadha 1999) for identification of hydrochemical processes, the values group into three sets based on the evolution of the leachate composition (Fig. 6). Set 1 is made up of a single solution that corresponds to the onset of the experiment. Set 2 shows a significant decrease in anion content (Cl<sup>-</sup> and SO<sub>4</sub><sup>2-</sup>) in the solution, whereas set 3 is characterised by a notable reduction in Na, K, Ca and Mg contents, reaching a generally stable situation where no more significant changes are observed (Fig. 6). The batch results are close to the starting value of the column experiment in Fig. 6, with the exception of samples ISG-5 and ISG-8, which also show anomalous behaviour here. This behaviour is interpreted as being partially related to their

exposure to rain, and thus, the plot of leaching results on a Chadha diagram could be a useful tool for distinguishing nonpristine ash samples. In addition, these two samples belong to the coarser group of samples, pointing out that the anomalous behaviour observed in the Chadha plot could be also related with the fact that finer ash presents a larger surface/volume ratio promoting the conditions for the formation of soluble salts on ash surface.

The element masses released in the column experiment are lower than in the batch tests (Table 3). These masses were estimated by interpolating values between analysed samples to complete the data for the total percolated volume. Variations between elements are due to the different physicochemical conditions during

**Fig. 5** Changes in the element concentrations, pH and SC of the ash leachate of ISG-3 ash sample from Grímsvötn 2011 eruption during the flow-through column experiment in deionised water. Ten grams of ash was leached in a flow-through column with 1000 ml (percolate volume) of deionised water pumped at 0.12 ml/min with ash-water contact time of around 150 min



the experiments. For the major elements, Si has the closest values for the two methods ( $8.60 \times 10^8$  g in batch vs.  $8.17 \times 10^8$  g in column). On the other hand, S and Cl have the largest differences ( $7.02 \times 10^9$  vs.  $9.73 \times 10^8$  g

for S and  $1.09 \times 10^9$  vs.  $1.40 \times 10^8$  g for Cl, for batch and column tests, respectively). Assuming that batch results reflect the maximum available elemental content of an ash, the column results corroborate their fast release into the environment

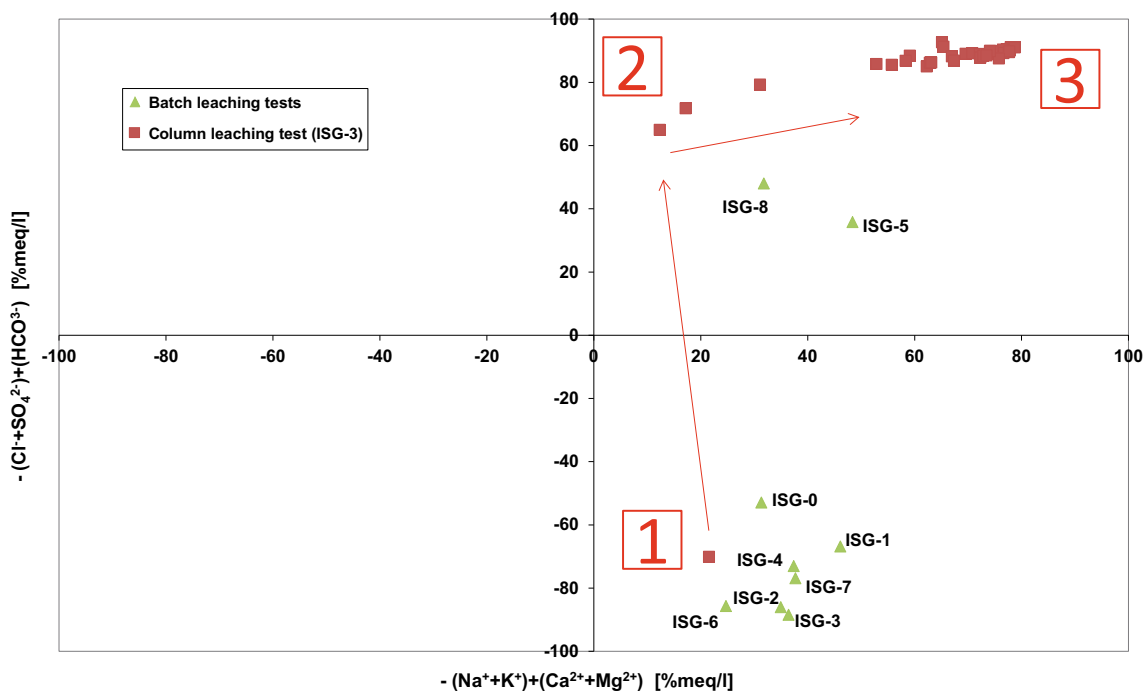


**Fig. 6** Chadha diagram (Chadha 1999) of the chemical compositions of the batch (1 g of volcanic ash was shaken with 10 ml of deionised water for 4 h) and column leachates (10 g of ash was leached in a flow-through column with 1000 ml of deionised water pumped at 0.12 ml/min). This plot shows the difference between divalent alkaline cations ( $Ca^{2+}$  and

$Mg^{2+}$ ) and monovalent alkaline cations ( $Na^+$  and  $K^+$ ) in milliequivalent (meq) percentage over the difference between weak ( $HCO_3^-$ ) and strong ( $Cl^-$  and  $SO_4^{2-}$ ) acid anions. Red numbers correspond to the different steps of the leaching process observed in the column test in sample ISG-3

for practically all the studied elements when ash interacts with water.

### Conclusions

The study of the ash generated during the May 2011 eruption of the Icelandic volcano Grímsvötn demonstrates the complementary nature of batch and column leaching experiments in the assessment of the environmental consequences of ejection of ash into the atmosphere and its later deposition on terrestrial and aqueous surfaces. Furthermore, it helps consolidate the methodology for the environmental study of volcanic ash, while at the same time providing new tools to distinguish pristine from nonpristine samples.

In this scenario, the main findings regarding the May 2011 eruption of Grímsvötn volcano reveal that Na, K, Ca, Mg, Si, Cl, S and F show the largest geochemical fluxes caused by the interaction of water and ash. Additionally, the significant amounts of some of these elements (Ca, S and Mg) together with P, Cl and Fe, which are usually considered as macro/micronutrients, demonstrate the fertilising potential of the May 2011 emitted ash. On the other hand, release of F highlights the possible environmental problems arising from ash fallout on land or into fresh water systems. It is noteworthy that the chemical release is maximal during the first few hours

of contact between tephra and water due to the dissolution of soluble salts from the ash surface. As time progresses, these constituents are exhausted, the release drops considerably, and elements are freed instead by the incongruent dissolution of the volcanic glass. In addition, the scarce presence of iron sulphide, which is very rare in juvenile ash, underlines the singularity of this sample collection.

**Acknowledgments** We gratefully acknowledge the assistance of ICTJA-CSIC labGEOTOP (infrastructure co-funded by ERDF-EU Ref. CSIC08-4E-001) and DRX (infrastructure co-funded by ERDF-EU Ref. CSIC10-4E-141) Surveys (J. Ibañez, J. Elvira and S. Alvarez) and the CCiTUB (SEM Unit) in the analytical work. Financial support was provided by the QUECA Project (MINECO, CGL2011-23307). We appreciate the invaluable comments of Dr. N. Olgun on a previous version of the manuscript. This study was carried out in the framework of the Research Consolidated Groups GEOPAM (Generalitat de Catalunya, 2014 SGR 869) and GEOVOL and the Associated Unit CSIC-UB UAGEPE (UA 285P01). We thank Prof. D. Gimeno for the collaboration in different aspects of this work. F. van Wyk de Vries is gratefully acknowledged for useful comments and improvement in English style. Field pictures were taken by Ó. Pérez.

### References

Agustsdottir AM, Brantley SL (1994) Volatile fluxes integrated over 4 decades at Grímsvötn volcano, Iceland. *J Geophys Res Solid Earth* 99:9505–9522. doi:10.1029/93jb03597

- Alfaro R, Brandsdóttir B, Rowlands DP, White RS, Gudmundsson MT (2007) Structure of the Grimsvotn central volcano under the Vatnajökull icecap. *Iceland Geophys J Int* 168:863–876. doi:10.1111/j.1365-246X.2006.03238.x
- Ayris PM, Delmelle P (2012) The immediate environmental effects of tephra emission. *Bull Volcanol* 74:1905–1936. doi:10.1007/s00445-012-0654-5
- Bagnato E et al (2013) Scavenging of sulphur, halogens and trace metals by volcanic ash: the 2010 Eyjafjallajökull eruption. *Geochimica Et Cosmochimica Acta* 103:138–160. doi:10.1016/j.gca.2012.10.048
- Bonadonna C et al. (2011) Tephra sedimentation during the 2010 Eyjafjallajökull eruption (Iceland) from deposit, radar, and satellite observations *Journal of Geophysical Research-Solid Earth* 116 doi: 10.1029/2011jb008462
- Brown RJ, Bonadonna C, Durant AJ (2012) A review of volcanic ash aggregation. *Phys Chem Earth* 45–46:65–78. doi:10.1016/j.pce.2011.11.001
- Casadevall TJ (1994) Volcanic ash and aviation safety; proceedings of the First international symposium on Volcanic ash and aviation safety. *USGS Bulletin* 2047:1–418
- Chadha DK (1999) A proposed new diagram for geochemical classification of natural waters and interpretation of chemical data *Hydrogeology Journal* 7:431–439 doi:10.1007/s100400050216
- Delmelle P, Lambert M, Dufrene Y, Gerin P, Oskarsson N (2007) Gas/aerosol-ash interaction in volcanic plumes: new insights from surface analyses of fine ash particles. *Earth Planet Sci Lett* 259:159–170. doi:10.1016/j.epsl.2007.04.052
- Duggen S, Olgun N, Croot P, Hoffmann L, Dietze H, Delmelle P, Teschner C (2010) The role of airborne volcanic ash for the surface ocean biogeochemical iron-cycle: a review. *Biogeosciences* 7:827–844. doi:10.5194/bg-7-827-2010
- EEA (2010) The European environment—state and outlook 2010: synthesis. Country assessments. Iceland. Population density. European Environment Agency, Copenhagen
- Fernandez-Turiel JL, Llorens JF, Lopez-Vera F, Gomez-Artola C, Morell I, Gimeno D (2000) Strategy for water analysis using ICP-MS. *Fresenius J Anal Chem* 368:601–606
- Fontijn K, Lachowycz SM, Rawson H, Pyle DM, Mather TA, Naranjo JA, Moreno-Roa H (2014) Late Quaternary tephrostratigraphy of southern Chile and Argentina. *Quat Sci Rev* 89:70–84. doi:10.1016/j.quascirev.2014.02.007
- Frogner P, Gislason SR, Oskarsson N (2001) Fertilizing potential of volcanic ash in ocean surface water. *Geology* 29:487–490
- Gislason SR et al. (2011) Characterization of Eyjafjallajökull volcanic ash particles and a protocol for rapid risk assessment *Proceedings of the National Academy of Sciences of the United States of America* 108: 7307–7312 doi:10.1073/pnas.1015053108
- Gislason SR, Oelkers EH (2003) Mechanism, rates, and consequences of basaltic glass dissolution: II. An experimental study of the dissolution rates of basaltic glass as a function of pH and temperature. *Geochimica Et Cosmochimica Acta* 67:3817–3832. doi:10.1016/s0016-7037(00)00176-5
- Gudmundsson MT, Sigmundsson F, Björnsson H (1997) Ice-volcano interaction of the 1996 Gjalp subglacial eruption, Vatnajökull, Iceland. *Nat* 389:954–957. doi:10.1038/40122
- Gudmundsson MT, Thordarson T, Höskuldsson A, Larsen G, Björnsson H, Prata FG, Oddsson B, Magnússon E, Högnadóttir T, Petersen GN, Hayward CL, Stevenson JA, Jónsdóttir I (2012) Ash generation and distribution from the April–May 2010 eruption of Eyjafjallajökull, Iceland. *Scientific Reports* 2:572. doi:10.1038/srep00572
- Guffanti M, Mayberry GC, Casadevall TJ, Wunderman R (2009) Volcanic hazards to airports. *Nat Hazards* 51:287–302. doi:10.1007/s11069-008-9254-2
- Horwell CJ, Baxter PJ (2006) The respiratory health hazards of volcanic ash: a review for volcanic risk mitigation. *Bull Volcanol* 69:1–24. doi:10.1007/s00445-006-0052-y
- Horwell CJ et al (2013) Physicochemical and toxicological profiling of ash from the 2010 and 2011 eruptions of Eyjafjallajökull and Grimsvotn volcanoes, Iceland using a rapid respiratory hazard assessment protocol. *Environ Res* 127:63–73. doi:10.1016/j.envres.2013.08.011
- Hreinsdóttir S et al (2014) Volcanic plume height correlated with magma-pressure change at Grimsvotn Volcano, Iceland. *Nat Geosci* 7:214–218. doi:10.1038/ngeo2044
- Jones MT, Gislason SR (2008) Rapid releases of metal salts and nutrients following the deposition of volcanic ash into aqueous environments. *Geochimica Et Cosmochimica Acta* 72:3661–3680. doi:10.1016/j.gca.2008.05.030
- Jude-Eton TC, Thordarson T, Gudmundsson MT, Oddsson B (2012) Dynamics, stratigraphy and proximal dispersal of supraglacial tephra during the ice-confined 2004 eruption at Grimsvotn Volcano Iceland. *Bull Volcanol* 74:1057–1082. doi:10.1007/s00445-012-0583-3
- Kerminen VM et al. (2011) Characterization of a volcanic ash episode in southern Finland caused by the Grimsvotn eruption in Iceland in May 2011 *Atmospheric Chemistry and Physics* 11:12227–12239 doi:10.5194/acp-11-12227-2011
- Kvietkus K, Sakalys J, Didzbalis J, Garbariene I, Spirkauskaitė N, Remeikis V (2013) Atmospheric aerosol episodes over Lithuania after the May 2011 volcano eruption at Grimsvotn, Iceland. *Atmos Res* 122:93–101. doi:10.1016/j.atmosres.2012.10.014
- Langmann B, Zaksek K, Hort M, Duggen S (2010) Volcanic ash as fertiliser for the surface ocean. *Atmos Chem Phys* 10:3891–3899
- Liu EJ, Cashman KV, Rust AC, Gislason SR (2015) The role of bubbles in generating fine ash during hydromagmatic eruptions. *Geology* 43(3):239–242
- Long CJ, Power MJ, Minckley TA, Hass AL (2014) The impact of Mt Mazama tephra deposition on forest vegetation in the Central Cascades, Oregon, USA *Holocene* 24:503–511. doi:10.1177/0959683613520258
- Olgun N, Duggen S, Andronico D, Kutterolf S, Croot PL, Giammanco S, Censi P, Randazzo L (2013) Possible impacts of volcanic ash emissions of Mount Etna on the primary productivity in the oligotrophic Mediterranean Sea: results from nutrient-release experiments in seawater. *Mar Chem* 152:32–42. doi:10.1016/j.marchem.2013.04.004
- Olgun N, Duggen S, Croot PL, Delmelle P, Dietze H, Schacht U, Oskarsson N, Siebe C, Auer A, Garbe-Schönberg D (2011) Surface ocean iron fertilization: the role of airborne volcanic ash from subduction zone and hot spot volcanoes and related iron fluxes into Pacific Ocean. *Global Biogeochemical Cycles* 25:GB4001. doi:10.1029/2009GB003761
- Olsson J, Stipp SLS, Dalby KN, Gislason SR (2013) Rapid release of metal salts and nutrients from the 2011 Grimsvotn, Iceland volcanic ash. *Geochimica Et Cosmochimica Acta* 123:134–149. doi:10.1016/j.gca.2013.09.009
- Oskarsson N, Sverrisdóttir G (2011) Chemical composition and texture of ash from the Grímsvötn 2011-eruption. Institute of Earth Sciences, University of Iceland, 2011, available online at: [http://earthice.hi.is/page/ies\\_GV2011\\_chemical](http://earthice.hi.is/page/ies_GV2011_chemical)
- Petersen GN, Björnsson H, Arason P, von Löwis S (2012) Two weather radar time series of the altitude of the volcanic plume during the May 2011 eruption of Grímsvötn, Iceland. *Earth Syst Sci Data* 4:121–127. doi:10.5194/essd-4-121-2012
- Rango T, Colombani N, Mastrocicco M, Bianchini G, Beccaluva L (2010) Column elution experiments on volcanic ash: geochemical implications for the main Ethiopian rift waters. *Water Air Soil Pollut* 208:221–233. doi:10.1007/s11270-009-0161-2
- Robock A (2000) Volcanic eruptions and climate. *Rev Geophys* 38:191–219. doi:10.1029/1998rg000054

- Rose WI (1977) Scavenging of volcanic aerosol by ash—atmospheric and volcanologic implications. *Geology* 5:621–624
- Ruggieri F et al (2012a) Contribution of volcanic ashes to the regional geochemical balance: the 2008 eruption of Chaiten volcano, Southern Chile. *Sci Total Environ* 425:75–88. doi:10.1016/j.scitotenv.2012.03.011
- Ruggieri F et al (2012b) Multivariate factorial analysis to design a robust batch leaching test to assess the volcanic ash geochemical hazard. *J Hazard Mater* 213:273–284. doi:10.1016/j.jhazmat.2012.01.091
- Ruggieri F, Saavedra J, Fernandez-Turiel JL, Gimeno D, Garcia-Valles M (2010) Environmental geochemistry of ancient volcanic ashes. *J Hazard Mater* 183:353–365. doi:10.1016/j.jhazmat.2010.07.032
- Sigmarrsson O, Haddadi B, Carn S, Moune S, Gudnason J, Yang K, Clarisse L (2013) The sulfur budget of the 2011 Grimsvotn eruption, Iceland. *Geophys Res Lett* 40:6095–6100. doi:10.1002/2013gl057760
- Sturkell E, Einarsson L, Sigmundsson F, Hreinsdottir S, Geirsson H (2003) Deformation of Grimsvotn volcano, Iceland: 1998 eruption and subsequent inflation *Geophysical Research Letters* 30 doi:10.1029/2002gl016460
- Taddeucci J et al. (2011) Aggregation-dominated ash settling from the Eyjafjallajokull volcanic cloud illuminated by field and laboratory high-speed imaging *Geology* 39:891–894 doi:10.1130/g32016.1
- Taylor HE, Lichte FE (1980) Chemical composition of Mount St. Helens volcanic ash. *Geophys Res Lett* 7:949–952. doi:10.1029/GL007i011p00949
- Tesche M et al. (2012) Volcanic ash over Scandinavia originating from the Grimsvotn eruptions in May 2011 *Journal of Geophysical Research-Atmospheres* 117 doi:10.1029/2011jd017090
- Thordarson T, Self S (2003) Atmospheric and environmental effects of the 1783–1784 Laki eruption: a review and reassessment *Journal of Geophysical Research-Atmospheres* 108 doi:10.1029/2001jd002042
- Weaire J, Manly R (1996) Chemical quality water studies in the Central Patagonian Region of Chile following the eruption of Volcan Hudson. *Hydrobiologia* 331:161–166
- Webster HN et al. (2012) Operational prediction of ash concentrations in the distal volcanic cloud from the 2010 Eyjafjallajokull eruption *Journal of Geophysical Research-Atmospheres* 117 doi:10.1029/2011jd016790
- Witham C, Webster H, Hort M, Jones A, Thomson D (2012) Modelling concentrations of volcanic ash encountered by aircraft in past eruptions. *Atmos Environ* 48:219–229. doi:10.1016/j.atmosenv.2011.06.073
- Witham CS, Oppenheimer C, Horwell CJ (2005) Volcanic ash-leachates: a review and recommendations for sampling methods. *J Volcanol Geotherm Res* 141:299–326. doi:10.1016/j.jvolgeores.2004.11.010